

## 基于 3,3',4,4'-四羧基偶氮苯构筑的三个金属配合物的合成、晶体结构及性质

陈小莉\* 崔华莉 杨 华 任宜霞 王记江 王 潇

(延安大学化学与化工学院, 陕西省反应工程重点实验室, 新能源新材料实验室, 延安 716000)

**摘要:** 在水热条件下利用  $H_4ddb$  配体合成了 3 个过渡金属配合物  $[Co_2(ddb)(phen)_2(H_2O)_6] \cdot 3H_2O$  (**1**),  $[Co(ddb)_{0.5}(bpy)_{0.5}(H_2O)_3]_n$  (**2**) 和  $[Ag(dpe)] \cdot 0.5(H_2ddb) \cdot H_2O$  (**3**) ( $H_4ddb=3,3',4,4'$ -四羧基偶氮苯,  $bpy=4,4'$ -联吡啶,  $dpe=1,2$ -二(4-吡啶基乙烯)), 并用元素分析、红外光谱、X 射线粉末衍射、X 射线单晶衍射对其进行了表征。配合物 **1** 为双核结构, 基于丰富的氢键作用扩展形成三维超分子网络结构。配合物 **2** 为基于钴离子通过  $ddb^{4-}$  配体以  $\mu_4:\eta^1, \eta^1, \eta^1, \eta^1$  的配位模式连接而成的二维网结构。配合物 **3** 是由  $Ag(I)$  离子与  $dpe$  配体形成的直链结构, 客体分子  $H_2ddb^{2-}$  通过氢键作用将其扩展为三维超分子结构。此外还研究了配合物 **1~3** 的荧光性质和热稳定性。

**关键词:** 过渡金属; 3,3',4,4'-四羧基偶氮苯; 晶体结构; 荧光

中图分类号: O614.81<sup>+</sup>2; O614.122

文献标识码: A

文章编号: 1001-4861(2018)12-2298-09

DOI: 10.11862/CJIC.2018.266

## Syntheses, Crystal Structures and Properties of Three Metal Complexes Based on 3,3',4,4'-Tetracarboxyazobenzene

CHEN Xiao-Li\* CUI Hua-Li YANG Hua REN Yi-Xia WANG Ji-Jiang WANG Xiao  
(School of Chemistry and Chemical Engineering, Shaanxi Key Laboratory of Chemical Reaction Engineering,  
Laboratory of New Energy & New Function Materials, Yan'an University, Yan'an, Shaanxi 716000, China)

**Abstract:** Three transition metal complexes based on  $H_4ddb$  ligand, namely  $[Co_2(ddb)(phen)_2(H_2O)_6] \cdot 3H_2O$  (**1**),  $[Co(ddb)_{0.5}(bpy)_{0.5}(H_2O)_3]_n$  (**2**) and  $[Ag(dpe)] \cdot 0.5(H_2ddb) \cdot H_2O$  (**3**). ( $H_4ddb=3,3',4,4'$ -tetracarboxyazobenzene,  $bpy=4,4'$ -pyridine,  $dpe=1,2$ -di(4-pyridyl)ethylene) have been synthesized and structurally characterized by elemental analyses, IR spectroscopy, powder X-ray diffraction and single-crystal X-ray diffraction analyses. Complex **1** is binuclear structure, which is linked into 3D supramolecular network through rich hydrogen bonding interactions. Complex **2** shows 2D network constructed from  $Co^{2+}$  ion cross-linked by  $ddb^{4-}$  ligands via  $\mu_4:\eta^1, \eta^1, \eta^1, \eta^1$  coordination mode. Complex **3** is linear chain structure based on  $Ag(I)$  ion and  $dpe$  ligands. Interestingly, the guest molecule  $H_2ddb^{2-}$  extends a 3D supramolecular structure of **3** through intermolecular hydrogen bonding interactions. In addition, the thermal stabilities and luminescence properties of **1~3** were also studied. CCDC: 1861508, **1**; 1861509, **2**; 1861510, **3**.

**Keywords:** transition metal; 3,3',4,4'-tetracarboxyazobenzene; crystal structure; luminescence

收稿日期: 2018-08-30。收修改稿日期: 2018-09-14。

国家自然科学基金(No.21763028)和延安大学科研计划项目(No.YDY2017-07)资助。

\*通信联系人。E-mail: chenxiaoli003@163.com; 会员登记号: S06N7138M1005。

## 0 Introduction

The crystal engineering of metal-organic frameworks (MOFs) have been attracted extensive attention, not only because of their fantastic topological structures but also promising properties in luminescence, magnetism, catalysis, gas absorption and separation and so on<sup>[1-7]</sup>. Although a variety of metal MOFs with desired structures and functions have been synthesized to date, rational control in the construction of polymers remains a great challenge in crystal engineering. In order to prepared MOFs with diverse structures and desired functionalities, judicious selection of appropriate polydentate organic ligands and metal ions is one of the most efficient strategies<sup>[8-11]</sup>. So many polycarboxylate ligands are often employed as bridging ligands to construct MOFs, due to their extension ability both in covalent bonding and in supramolecular interactions (H-bonding and aromatic stacking)<sup>[12-15]</sup>.

As a member of polycarboxylate ligands, 3,3',4,4'-tetracarboxyazobenzene ( $H_4ddb$ ) has four carboxyl groups that may be completely or partially deprotonated, and can provide hydrogen bond donors and acceptors, which makes it a wonderful candidate for the construction of supramolecular networks depending upon the number of deprotonated carboxylate groups. Therefore,  $H_4ddb$  may be an excellent candidate for the construction of multidimensional coordination polymers.

However, to the best of our knowledge,  $ddb$ -metal complex have rarely been reported<sup>[16-21]</sup>, and much work is still necessary to understand the coordination chemistry of  $ddb^{4-}$  ligand. We also notice that the introduction of N-containing auxiliary ligands such as 1,10-phenanthroline (phen), 4,4'-bipyridine (bpy), 1,2-bis(4-pyridyl)ethane (bpe) or 1,2-di(4-pyridyl)ethylene (dpe) via adjustment of the carboxylate bridging mode into the system may lead to new structural evolution and fine-tuning the structural motif of the complexes<sup>[22-25]</sup>. With the aim of understanding the coordination chemistry of them and studying the influence on the framework structure of the complexes, we have recently engaged in the research of this kind of complex.

Luckily, we have now obtained three complexes,  $[Co_2(ddb)(phen)_2(H_2O)_6] \cdot 3H_2O$  (**1**),  $[Co(ddb)_{0.5}(bpy)_{0.5}(H_2O)_3]_n$  (**2**) and  $[Ag(dpe)] \cdot 0.5(H_2ddb) \cdot H_2O$  (**3**). Herein we reported their syntheses, structures, thermal stabilities and luminescent properties.

## 1 Experimental

### 1.1 Reagents and physical measurements

All chemicals and reagents were used as received from commercial sources without further purification. All reactions were carried out under hydrothermal conditions. Elemental analyses (C, H, N) were determined with a Elementar Vario EL III elemental analyzer. IR spectra were recorded as KBr pellets on a Bruker EQUINOX55 spectrophotometer in the 4 000~400  $cm^{-1}$  region. Fluorescence spectra were performed on a Hitachi F-4500 fluorescence spectro-photometer at room temperature. Thermogravimetric analyses (TGA) were performed in a nitrogen atmosphere with a heating rate of 10  $^{\circ}C \cdot min^{-1}$  with a NETZSCHSTA 449C thermogravimetric analyzer. The X-ray powder diffraction pattern (XRD) was recorded with a Rigaku D/Max III diffractometer operating at 40 kV and 30 mA using  $Mo K\alpha$  radiation ( $\lambda=0.15418$  nm) in the range of  $5^{\circ} \sim 50^{\circ}$ .

### 1.2 Synthesis of $[Co_2(ddb)(phen)_2(H_2O)_6] \cdot 3H_2O$ (**1**)

A mixture of  $Co(Ac)_2 \cdot 4H_2O$  (24.9 mg, 0.1 mmol),  $H_4ddb$  (35.8 mg, 0.1 mmol), phen (19.8 mg, 0.1 mmol) and water (10 mL) was stirred and adjusted to pH 6.5 with 0.5  $mol \cdot L^{-1}$  NaOH solution, then sealed in a 25 mL Teflon-lined stainless steel container, which was heated to 160  $^{\circ}C$  for 96 h. Then cooling to room temperature at a rate of 5  $^{\circ}C \cdot h^{-1}$ . Brown crystals were obtained in ca. 53% yield based on Co. Anal. Calcd. for  $C_{40}H_{40}Co_2N_6O_{17}$ (%): C, 48.30; H, 4.05; N, 8.45. Found(%): C, 48.49; H, 3.72; N, 8.45. FI-IR (KBr,  $cm^{-1}$ ): 3 394(s), 3 072(s), 1 628(m), 1 553(s), 1 486(m), 1 422(s), 1 209(w), 1 140(w), 1 070(w), 922(w), 845(m), 801(m), 726(m), 671(w).

### 1.3 Synthesis of $[Co(ddb)_{0.5}(bpy)_{0.5}(H_2O)_3]_n$ (**2**)

The brown crystals of **2** were prepared by a similar method used in the synthesis of **1** except that

phen was replaced by bpy (Yield: 45% based on Co). Anal. Calcd. for  $C_{13}H_{13}CoN_2O_7$ (%): C, 42.41; H, 3.56; N, 7.61. Found(%): C, 42.43; H, 3.52; N, 7.63. FI-IR (KBr,  $cm^{-1}$ ): 3 387 (s), 3 090 (s), 1 610 (m), 1 564(s), 1 473(m), 1 409(s), 1 202(w), 1 056(w), 1 102(w), 906 (w), 845(m), 804(m), 720(m), 678(w).

#### 1.4 Synthesis of $\{[Ag(dpe)] \cdot 0.5(H_2ddb) \cdot H_2O\}_n$ (**3**)

The colorless crystals of **3** were prepared by a similar method used in the synthesis of **1** except that phen was replaced by dpe and  $Co(Ac)_2 \cdot 4H_2O$  (24.9 mg, 0.1 mmol) was replaced by  $AgNO_3$  (16.9 mg, 0.1 mmol) (Yield: 39% based on Ag). Anal. Calcd. for  $C_{20}H_{16}AgN_3O_5$ (%): C, 49.61; H, 2.91; N, 8.68. Found (%): C, 49.67; H, 2.85; N, 8.65. FI-IR (KBr,  $cm^{-1}$ ): 3 429(s), 3 037(w), 1 701(s), 1 607(s), 1 495(s), 1 357 (s), 1 240(w), 1 202(m), 1 068 (w), 969 (m), 831 (m), 771(w), 617(w), 547(m).

#### 1.5 X-ray crystallography

Intensity data were collected on a Bruker Smart APEX II CCD diffractometer with graphite-monochromated Mo  $K\alpha$  radiation ( $\lambda=0.071\ 073\ nm$ ) at room temperature. Empirical absorption corrections were applied using the SADABS program<sup>[26a]</sup>. The structures were solved by direct methods and refined by the full-matrix least-squares based on  $F^2$  using SHELXTL-97 program<sup>[26b]</sup>. In **3**, one dpe molecule and two oxygen atoms were split into two site with an occupancy ratio 0.5:0.5 for C6/C6A, C7/C7A, O3/O3A and O6/O6A. All non-hydrogen atoms were refined anisotropically and hydrogen atoms of organic ligands were generated geometrically. Crystal data and structural refinement parameters for **1**~**3** are summarized in Table 1, selected bond distances and bond angles are listed in Table 2.

CCDC: 1861508, **1**; 1861509, **2**; 1861510, **3**.

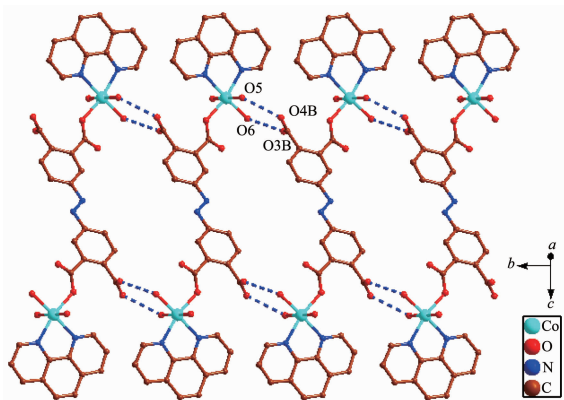
Table 1 Crystal data and structural refinement parameters for the title complexes **1**~**3**

Complex	<b>1</b>	<b>2</b>	<b>3</b>
Empirical formula	$C_{40}H_{40}Co_2N_6O_{17}$	$C_{13}H_{13}CoN_2O_7$	$C_{20}H_{16}AgN_3O_5$
Formula weight	994.64	368.18	486.23
Crystal system	Monoclinic	Triclinic	Triclinic
Space group	$C2/c$	$P\bar{1}$	$P\bar{1}$
$a / nm$	2.179 4(2)	0.598 02(5)	0.736 92(11)
$b / nm$	0.800 25(9)	0.874 66(7)	1.143 28(17)
$c / nm$	2.595 4(3)	1.418 60(11)	1.243 91(19)
$\alpha / (^\circ)$		101.296 0(10)	75.985(2)
$\beta / (^\circ)$	108.050(2)	92.210 0(10)	82.837(2)
$\gamma / (^\circ)$		100.118 0(10)	79.311(2)
$V / nm^3$	4.303 8(8)	0.714 28(10)	0.995 7(3)
$Z$	4	2	2
$D_c / (g \cdot cm^{-3})$	1.53	1.712	1.622
$\theta$ range for data / $(^\circ)$	1.65~28.43	1.47~25.50	1.69~25.50
Absorption coefficient / $mm^{-1}$	0.853	1.242	1.049
Crystal size / mm	0.34×0.29×0.26	0.30×0.28×0.27	0.31×0.27×0.25
$F(000)$	2 036	376	488
Reflection collected	12 972	3 731	5 162
Unique reflection ( $R_{int}$ )	5 266 (0.039 2)	2 636 (0.009 7)	3 610 (0.012 5)
Observed reflection [ $I > 2\sigma(I)$ ]	3 582	2 533	3 149
Limiting-indices	$-22 \leq h \leq 29,$ $-10 \leq k \leq 10,$ $-34 \leq l \leq 34$	$-6 \leq h \leq 7,$ $-10 \leq k \leq 10,$ $-17 \leq l \leq 14$	$-8 \leq h \leq 7,$ $-13 \leq k \leq 9,$ $-14 \leq l \leq 15$
Goodness-of-fit (on $F^2$ )	1.098	1.198	1.107
$R_1, wR_2$ [ $I > 2\sigma(I)$ ]	0.051 7, 0.113 7	0.024 2, 0.072 2	0.042 9, 0.107 9
$R_1, wR_2$ (all data)	0.090 7, 0.140 3	0.026 9, 0.084 2	0.050 0, 0.111 8

Complex 1					
Co(1)-O(1)	0.207 2(2)	Co(1)-O(6)	0.209 8(2)	Co(1)-O(5)	0.210 1(3)
Co(1)-O(7)	0.212 9(2)	Co(1)-N(3)	0.212 0(3)	Co(1)-N(2)	0.215 5(3)
O(1)-Co(1)-O(6)	95.52(9)	O(1)-Co(1)-O(5)	90.68(10)	O(5)-Co(1)-N(3)	94.69(10)
O(1)-Co(1)-O(7)	92.74(9)	O(1)-Co(1)-N(2)	167.25(10)	O(6)-Co(1)-N(2)	97.22(10)
O(6)-Co(1)-O(5)	90.99(10)	O(6)-Co(1)-O(7)	83.86(9)	O(5)-Co(1)-N(2)	89.17(11)
O(1)-Co(1)-N(3)	89.87(9)	O(5)-Co(1)-O(7)	174.07(10)	N(3)-Co(1)-N(2)	77.44(11)
O(6)-Co(1)-N(3)	172.12(10)	N(3)-Co(1)-O(7)	90.17(10)	O(7)-Co(1)-N(2)	88.56(10)
Complex 2					
Co(1)-O(1)	0.201 92(15)	Co(1)-O(7)	0.206 55(17)	Co(1)-O(5)	0.208 18(16)
Co(1)-O(6)	0.209 25(15)	Co(1)-N(2)	0.217 18(17)	Co(1)-O(3A)	0.219 89(13)
O(1)-Co(1)-O(7)	173.42(7)	O(1)-Co(1)-O(5)	86.64(7)	O(7)-Co(1)-O(5)	88.93(7)
O(1)-Co(1)-O(6)	93.77(7)	O(7)-Co(1)-O(6)	90.77(7)	O(5)-Co(1)-O(6)	178.62(6)
O(1)-Co(1)-N(2)	90.10(7)	O(7)-Co(1)-N(2)	85.04(7)	O(5)-Co(1)-N(2)	90.04(6)
O(6)-Co(1)-N(2)	91.28(6)	O(1)-Co(1)-O(3A)	95.47(6)	O(7)-Co(1)-O(3A)	89.52(7)
O(5)-Co(1)-O(3A)	91.73(6)	O(6)-Co(1)-O(3A)	86.92(6)	N(2)-Co(1)-O(3A)	174.25(6)
Complex 3					
Ag(1)-N(1)	0.215 3(3)	Ag(1)-N(2)	0.215 5(3)		
N(1)-Ag(1)-N(2)	172.02(12)				

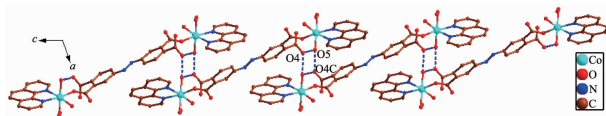
Scheme 1 Coordination modes of ddb<sup>4-</sup> in **1**~**2**

monodentately. Although  $\text{ddb}^{4-}$  ion participate in the coordination, two benzene rings of  $\text{ddb}^{4-}$  ion have not been distorted, and the dihedral angle between the two phenyl rings is  $0^\circ$  for **1**. On the basis of the connection mode, each pair of  $\text{Co(II)}$  ions are bridged by two carboxylate groups from one  $\text{ddb}^{4-}$  ligand to form a binuclear structure with the  $\text{Co1} \cdots \text{Co1}$  distances of 1.626 8 nm. The binuclear structure are linked by the hydrogen bonding interactions ( $\text{O5} \cdots \text{O4B}$ , 0.284 8(3) nm;  $\text{O6} \cdots \text{O3B}$ , 0.269 6 nm) generating a 1D double-chain (Fig.2). The adjacent double-chain recognizes each other to generate a 2D bilayer supramolecular network via hydrogen bonding interactions ( $\text{O5} \cdots \text{O4}$ , 0.284 8(3) nm;  $\text{O5} \cdots \text{O4C}$ , 0.277 5 nm), which is further developed into 3D supramolecular structure by hydrogen bonding interactions ( $\text{O7} \cdots \text{O2}$  0.275 5 nm,  $\text{O6} \cdots \text{O2}$  0.264 3(3) nm,  $\text{O7} \cdots \text{O8}$  0.279 1(6) nm,  $\text{O7} \cdots \text{O8A}$  0.258 7(8) nm,  $\text{O8} \cdots \text{O3}$  0.272 9 nm,  $\text{O9} \cdots \text{O3}$  0.283 0 nm, Fig.3).



All H atoms are omitted for clarity; Symmetry codes: B:  $x, -1+y, z$

Fig.2 View of 1D double-chain of **1** formed by hydrogen bonding interactions

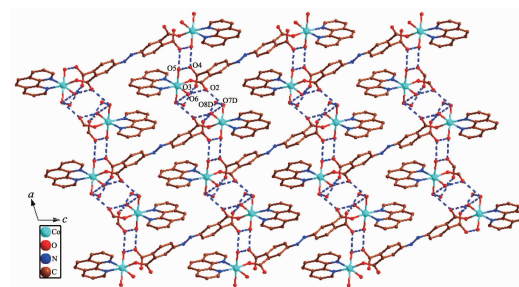


All H atoms are omitted for clarity; Symmetry codes: C:  $0.5-x, 1.5+y, 0.5-z$

Fig.3 View of 2D bilayer supramolecular network of **1** via hydrogen bonding interactions along  $b$ -axis

## 2.2 Structure description of complex 2

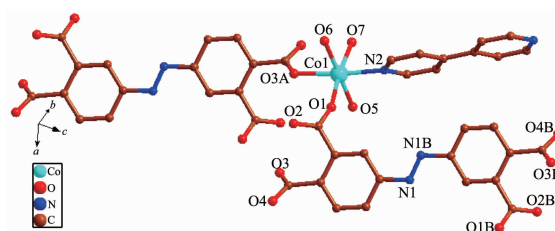
To further examine the influence of the auxiliary ligands on the structure of **1**, a longer bridge ligand



All H atoms are omitted for clarity; Symmetry codes: D:  $2-x, 3-y, -z$

Fig.4 View of 3D supramolecular architecture of **1** based on hydrogen bonding interaction along  $b$ -axis

bpy is used instead of phen. Consequently, a novel 2D polymeric network was obtained. The asymmetric unit of **2** contains one  $\text{Co(II)}$  atom, a half  $\text{ddb}^{4-}$  ligand, a half bpy ligand and three coordinated water molecules (Fig.5). Each  $\text{Co1}$  atom is six coordinated by one nitrogen atom ( $\text{Co1-N2}$  0.217 82(17) nm) from one bpy ligand, two carboxylate group oxygen atoms from two  $\text{ddb}^{4-}$  ligands and three water molecules. The bond lengths of  $\text{Co-O}$  are comparable to the published ones<sup>[28]</sup>, varying between 0.201 92(15) and 0.219 89(13) nm. The coordination geometry of  $\text{Co1}$  center can be described as a distorted octahedral geometry.



All H atoms are omitted for clarity; Symmetry codes: A:  $2-x, -y, -z$ ; B:  $2-x, -y, 1-z$

Fig.5 Coordination environment of  $\text{Co(II)}$  ion in **2**

In **2**,  $\text{H}_4\text{ddb}$  are completely deprotonated and adopts a  $\mu_4:\eta^1, \eta^1, \eta^1, \eta^1$  coordination mode (Scheme 1b). Four carboxylate groups adopt a bridging monodentate coordination mode connecting four  $\text{Co(II)}$  ions (Scheme 1b). Based on the connection mode, a pair of  $\text{Co(II)}$  ions are bridged by four carboxylate oxygen atoms from two  $\text{ddb}^{4-}$  ions to form a 14-membered ring  $\{\text{Co}_2\text{O}_4\text{C}_8\}$  (ring a) with the  $\text{Co1} \cdots \text{Co1}$  distance of 0.646 1 nm. Meanwhile, four  $\text{Co(II)}$  ions are also bridged by two  $\text{ddb}^{4-}$  ions and two bpy ligands to form a 46-membered ring  $\{\text{Co}_4\text{O}_4\text{N}_8\text{C}_{30}\}$  (ring b) containing a type



of pore with size of ca.  $2.481\ 8\ \text{nm} \times 2.520\ 8\ \text{nm}$  based on the distances of  $\text{Co1} \cdots \text{Co1}$  and  $\text{C1} \cdots \text{C1}$ . Interestingly, these 14-member and 46-membered rings were arranged alternately to form a 2D network (Fig.6). Two adjacent 2D networks are packed into 3D supramolecular structure by the hydrogen bonding interactions ( $\text{O5D} \cdots \text{O4C}$   $0.266\ 3\ \text{nm}$ ,  $\text{O7D} \cdots \text{O2C}$   $0.289\ 4\ \text{nm}$ ,  $\text{O6E} \cdots \text{O3C}$   $0.274\ 3\ \text{nm}$ ,  $\text{O6E} \cdots \text{O2}$   $0.259\ 3\ \text{nm}$ ,  $\text{O5D} \cdots \text{O6E}$   $0.284\ 6\ \text{nm}$ , Fig.7).

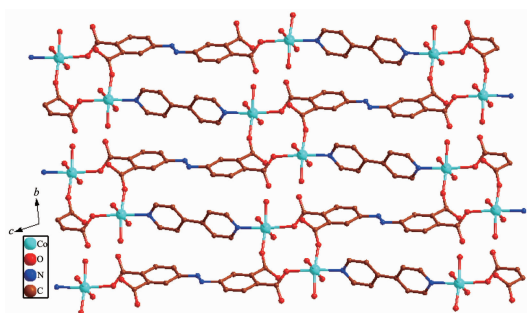
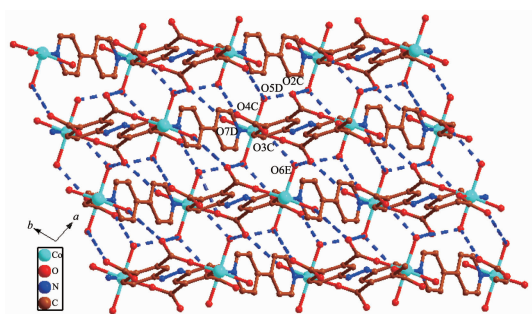


Fig.6 View of 2D network of **2** along *a*-axis



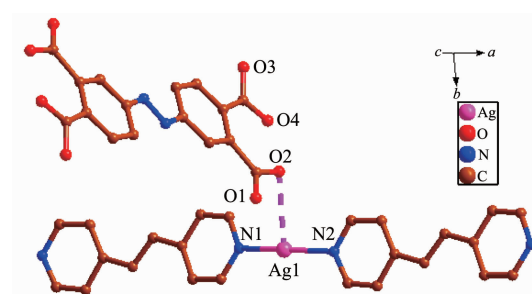
All H atoms are omitted for clarity; Symmetry codes: C:  $2-x, 1-y, 3-z$ ; D:  $x, 1+y, 2+z$ ; E:  $1-x, 1-y, 2-z$

Fig.7 View of 3D supramolecular architecture based on hydrogen bonding interaction along *c*-axis

### 2.3 Structure description of complex **3**

The asymmetric unit of **3** has one independent Ag(I) ion, one dpe ligand, a half free  $\text{H}_2\text{ddb}^{2-}$  ion and one lattice water molecule (Fig.8). Ag1 center coordinated with two nitrogen atoms (N1, N2) from two different dpe ligands ( $\text{Ag1-N2}$   $0.215\ 5(3)\ \text{nm}$ ,  $\text{Ag1-N1}$   $0.215\ 3(3)\ \text{nm}$ ) to form a slightly distorted linear geometry. However, the distance of  $0.283\ 9\ \text{nm}$  between Ag1-O2 suggests a non-negligible interaction between them. Thus, the coordination polyhedron of Ag(I) ion can also be described as a T-shaped coordination geometry. The  $\text{N1-Ag1-N2}$  bond angle is  $172.02^\circ$ , and the three atoms almost in a line. The pyridyl rings of

dpe ligand are non-coplanar with a dihedral angle of  $7.18^\circ$  and the  $\text{Ag1} \cdots \text{Ag1}$  separation based on dpe ligand is  $1.364\ 5\ \text{nm}$ . Hence, the dpe ligands bridge Ag1 centers to form 1D linear chain. The  $\text{Ag1} \cdots \text{Ag1}$  distance between two parallel linear chains is  $0.321\ 0\ \text{nm}$ , which is less than the van der Waals contact whose distance is  $0.340\ \text{nm}$ , illustrating the existence of argentophilic interactions between Ag(I) ions. Based on the argentophilic interactions between Ag(I) ions, the adjacent linear chains form a 1D double chain structure. Interestingly, the adjacent double chains interact with each other to generate a 2D supramolecular network through the  $\pi \cdots \pi$  stacking interactions with an edge-to-edge distance of  $0.338\ 7\ \text{nm}$  between two pyridine rings of dpe ligands and  $0.337\ 0, 0.338\ 8\ \text{nm}$  between the pyridine ring of dpe ligand and the double bonds of dpe ligand, respectively (Fig.9). These kinds of  $\pi \cdots \pi$  stacking interactions are in an alternate fashion and consolidate the stacked arrangement. The adjacent 2D structures further form a 3D supramolecular structure through  $\text{O-H} \cdots \text{O}$  hydrogen bonds ( $\text{O6A} \cdots \text{O4}$   $0.289\ 9\ \text{nm}$ ,  $\text{O5} \cdots \text{O3}$   $0.288\ 4\ \text{nm}$ ,  $\text{O6B} \cdots \text{O6A}$   $0.254\ 7\ \text{nm}$ ,  $\text{O5} \cdots \text{O6}$   $0.285\ 0\ \text{nm}$ ,  $\text{O6A} \cdots \text{O6B}$   $0.270\ 9\ \text{nm}$ ) and  $\text{Ag} \cdots \text{O}$  weak interactions ( $\text{Ag1A} \cdots \text{O1}$   $0.276\ 0\ \text{nm}$ ,  $\text{Ag1} \cdots \text{O2}$   $0.283\ 9\ \text{nm}$ , Fig.10).



All H atoms are omitted for clarity

Fig.8 Coordination environment of Ag(I) ion in **3**

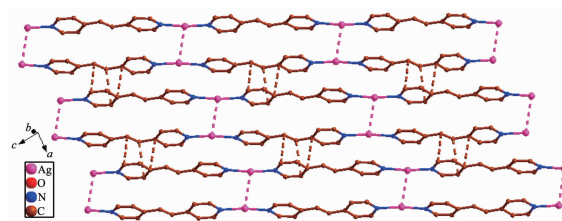
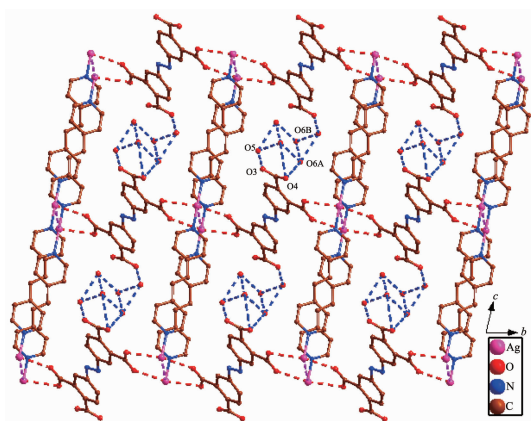


Fig.9 View of 2D supramolecular network of **3** via  $\text{Ag} \cdots \text{Ag}$  interactions and  $\pi \cdots \pi$  stacking interactions



All H atoms are omitted for clarity; Symmetry codes: A:  $2-x$ ,  $1-y$ ,  $1-z$ ; B:  $2-x$ ,  $1-y$ ,  $2-z$

Fig.10 View of 3D supramolecular structure of **3** based on hydrogen bonding interaction and  $\text{Ag}\cdots\text{O}$  weak interactions

## 2.2 IR Spectra of **1** and **2**

In the FT-IR spectra, the absorption bands in the region of  $3\,387\sim3\,429\text{ cm}^{-1}$  may attribute to the stretching vibrations of O-H and N-H. The bands in the region  $3\,037\sim3\,090\text{ cm}^{-1}$  can be ascribed to C-H stretching vibrations of the benzene ring<sup>[29]</sup>. The absence of the absorption bands at  $1\,730\sim1\,690\text{ cm}^{-1}$  in **1** and **2** indicates the  $\text{H}_4\text{ddb}$  ligand adopts the complete deprotonated  $\text{ddb}^{4-}$  form, which is consistent with the X-ray structural analysis. The bands in the region of  $1\,578\sim1\,628\text{ cm}^{-1}$  for **1~3** can be assigned to the  $\text{N}=\text{N}$  stretching vibrations. The asymmetric stretching vibrations of the carboxylate groups ( $\nu_{\text{as}}$ ) were observed at  $1\,553$ ,  $1\,564$  and  $1\,495\text{ cm}^{-1}$ , and the symmetric stretching vibration ( $\nu_{\text{s}}$ ) of the carboxylate groups were observed at  $1\,422$ ,  $1\,409$  and  $1\,357\text{ cm}^{-1}$ , respectively<sup>[30]</sup>. The separation  $\Delta\nu(\text{COO})$  between the  $\nu_{\text{as}}(\text{COO})$  and  $\nu_{\text{s}}(\text{COO})$  band for **1~3** are  $131$ ,  $155$  and  $138\text{ cm}^{-1}$ , which is smaller than  $200\text{ cm}^{-1}$ , indicating that the carboxyl groups are coordinated in bridging mode<sup>[31]</sup>.

## 2.3 Luminescent properties

The photoluminescence properties of complexes **1~3** were examined at room temperature, and the emission spectra are shown in Fig.11. The  $\text{H}_4\text{ddb}$  ligand exhibited one very weak emission band at  $470\text{ nm}$  upon excitation at  $294\text{ nm}$ . Upon excitation of

solid samples of **1~3** at  $284\text{ nm}$ , these complexes showed one emission peak at  $421\text{ nm}$  for **1**,  $438\text{ nm}$  for **2**,  $410\text{ nm}$  for **3**. In comparison with  $\text{H}_4\text{ddb}$  ligand, the emission peaks of complexes **1~3** were blue-shifted, which may be due to the  $\pi^*\rightarrow\pi$  intraligand fluorescence because of close resemblance to the emission band of  $\text{H}_4\text{ddb}$  ligand<sup>[32]</sup>. By comparing the emission spectra of **1~3** and the free ligand, we can conclude that the enhancement of luminescence in **1~3** may be attributed to the ligation of ligand to the metal center, which effectively increases the rigidity and reduces the loss of energy by radiationless decay<sup>[33-34]</sup>.

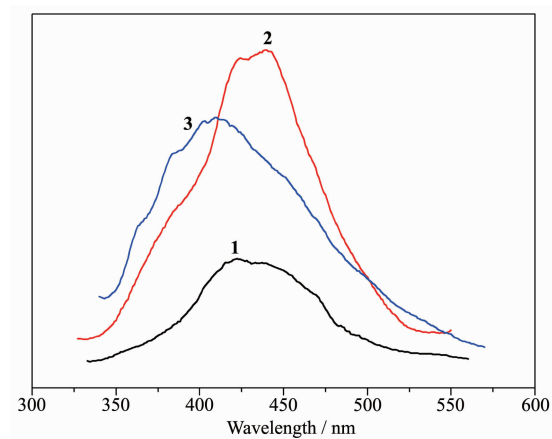


Fig.11 Emission spectra of **1~3** in the solid state at room temperature

## 2.4 Thermal properties and PXRD measurement of complexes **1~3**

To study the thermal stabilities of these complexes, thermal gravimetric analysis (TGA) were performed. The TG curve of **1~3** are shown in Fig.12. Complex **1** first lost its coordinated and lattice water molecule below  $210\text{ }^{\circ}\text{C}$  (Obsd.  $14.68\%$ , Calcd.  $14.52\%$ ). Then **1** was relatively stable up to  $210\sim345\text{ }^{\circ}\text{C}$ . The second weight loss is  $74.49\%$  in the temperature range of  $345\sim400\text{ }^{\circ}\text{C}$  corresponding to the decomposition of  $\text{ddb}^{4-}$  and phen ligands (Calcd.  $75.23\%$ ). Complex **2** first lost its coordinated water molecules below  $225\text{ }^{\circ}\text{C}$  (Obsd.  $14.88\%$ , Calcd.  $14.67\%$ ). Then **2** was relatively stable up to  $225\sim320\text{ }^{\circ}\text{C}$ , followed by a continuously two-step weight loss of  $73.41\%$  from  $320$  to  $515\text{ }^{\circ}\text{C}$  (Calcd.  $72.42\%$ ), corresponding to the loss of  $\text{ddb}^{4-}$  and phen ligands. The remaining weight of  $12.69\%$  is the final product  $\text{CoO}$  (Calcd.  $12.91\%$ ). The TG curve

of **3** showed an initial weight loss of 3.69% below 130 °C corresponding to the removal of lattice water

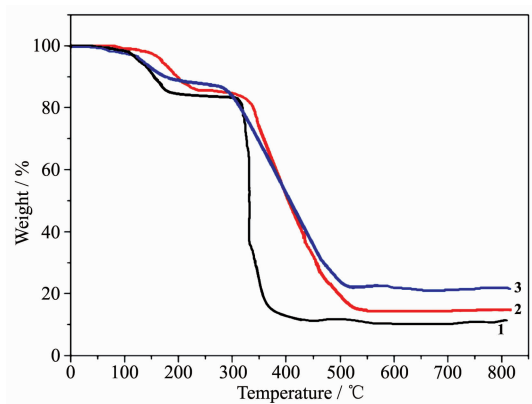


Fig.12 TGA curves of complexes **1~3**

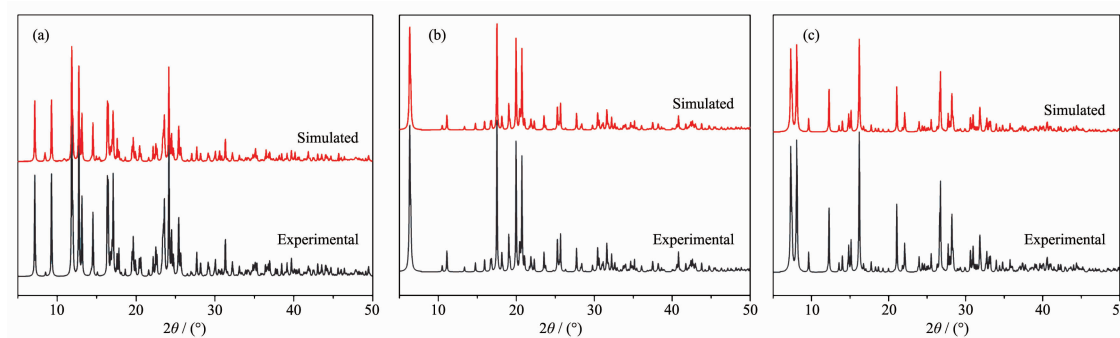


Fig.13 PXRD patterns of complexes **1** (a), **2** (b) and **3** (c)

### 3 Conclusions

In summary, we succeeded in getting access to three transition metal complexes based on 3,3',4,4'-tetracarboxyazobenzene and different auxiliary ligands through hydrothermal method. Complex **1** is binuclear structure. Complex **2** shows 2D network constructed from  $\text{Co}^{2+}$  ion cross-linked by  $\text{ddb}^{4-}$  and bpy ligand. Complex **3** is linear chain structure. Interestingly, the guest molecule  $\text{ddb}^{4-}$  exists in the structure and extends a 3D supramolecular structure through hydrogen bonding,  $\text{Ag} \cdots \text{Ag}$  and  $\text{Ag} \cdots \text{O}$  interactions. Different structures of complexes **1~3** indicate that the  $\text{ddb}^{4-}$  ligand has the ability of adjusting its coordination modes and configurations in different reaction systems. Furthermore, the  $\pi \cdots \pi$  stacking interactions probably play a crucial role to the arrangement and stability of the chain structure, which influence the final supramolecular structures together with abundant hydrogen-bond interactions.

molecules (Calcd. 3.72%). Then **3** was stable up to 260 °C and followed by the weight loss in the range of 260~490 °C, assigned to the decomposition of  $\text{ddb}^{4-}$  and dpe ligands (Calcd. 73.18%, Obsd. 72.57%). The remaining weight of 23.68% is  $\text{Ag}_2\text{O}$  that is in agreement with the calculated value of 23.76%.

In order to confirm the phase purity of the bulk materials, powder X-ray diffraction (PXRD) patterns were measured at room temperature. The PXRD experimental and computer-simulated patterns of all of them are shown in Fig.13. The peaks of the simulated and experimental PXRD patterns are in good agreement with each other, confirming the phase purities of **1~3**.

### References:

- [1] Yang X, Xu Q. *Cryst. Growth Des.*, **2017**,**17**:1450-1455
- [2] Kreno L E, Leong K, Farha O K, et al. *Chem. Rev.*, **2012**, **112**:1105-1125
- [3] Gil-Hernández B, Savvin S, Makhloufi G, et al. *Inorg. Chem.*, **2015**,**54**:1597-1605
- [4] Ding L G, Yao B J, Jiang W L, et al. *Inorg. Chem.*, **2017**, **56**:2337-2344
- [5] Zhao X L, Sun W Y. *CrystEngComm*, **2014**,**16**:3247-3258
- [6] Pang J, Jiang F, Wu M, et al. *Chem. Commun.*, **2014**,**50**: 2834-2836
- [7] Zhang Y B, Furukawa H, Yaghi O M, et al. *J. Am. Chem. Soc.*, **2015**,**137**:2641-2650
- [8] Zhao J, Wang Y N, Dong W W, et al. *Chem. Commun.*, **2015**, **51**:9479-9482
- [9] Gai Y L, Jiang F L, Hong M C, et al. *Cryst. Growth Des.*, **2014**,**14**:1010-1017
- [10] Li X Z, Li M A, Li Z, et al. *Angew. Chem. Int. Ed.*, **2008**, **47**:6371-6374
- [11] Cunha D, Yahia M B, Hall S, et al. *Chem. Mater.*, **2013**,**25**:



- 2767-2776
- [12]Patra R, Titi H M, Goldberg I. *CrystEngComm*, **2013**,**15**:2853-2862
- [13]Pan L, Liu H, Lei X, et al. *Angew. Chem. Int. Ed.*, **2003**,**42**:542-546
- [14]Habib H A, Sanchiz J, Janiak C. *Dalton Trans.*, **2008**:4877-4884
- [15]Sun D, Han L L, Yuan S, et al. *Cryst. Growth Des.*, **2013**,**13**:377-385
- [16]Wang C C, Jing H P, Zhang Y Q, et al. *Transition Met. Chem.*, **2015**,**40**:573-584
- [17]Wang J, Lu L, Wu W P, et al. *Synth. React. Inorg. Met.-Org. Nano-Met. Chem.*, **2012**,**42**:25-29
- [18]Wang J, Lu L, Wu W P, et al. *J. Chem. Res.*, **2011**,**35**:424-427
- [19]Wang J, Lu L, Wu W P, et al. *Synth. React. Inorg. Met.-Org. Nano-Met. Chem.*, **2013**,**43**:791-794
- [20]Wang J, Lu L, Wu W P, et al. *Synth. React. Inorg. Met.-Org. Nano-Met. Chem.*, **2012**,**42**:1217-1221
- [21]Lu L, Wang J, Bai J W, et al. *Cryst. Res. Technol.*, **2008**,**43**:1327-1330
- [22]Lightfoot P, Snedden A. *J. Chem. Soc. Dalton Trans.*, **1999**:3549-3551
- [23]Sun C Y, Li L C, Jin L P. *Polyhedron*, **2006**,**25**:3017-3024
- [24]Lee S W, Kim H J, Lee Y K, et al. *Inorg. Chim. Acta*, **2003**,**353**:151-158
- [25]Ahmad M, Sharma M K, Das R, et al. *Cryst. Growth Des.*, **2012**,**12**:1571-1578
- [26](a)Sheldrick G M. *SADABS*, University of Göttingen, Germany, **1996**.  
(b)Sheldrick G M. *SHELXS-97 and SHELXL-97, Program for X-ray Crystal Structure Solution and Refinement*, Göttingen University, Germany, **1997**.
- [27]WANG Li(王莉), KGAN Quan-Peng(康全鹏), HAO Jing(郝静), et al. *Chinese J. Inorg. Chem.*(无机化学学报), **2018**,**34**(3):525-533
- [28]LIU Ji-Wei(刘继伟). *Chinese J. Inorg. Chem.*(无机化学学报), **2017**,**33**(4):705-712
- [29]Chen S, Fan R Q, Sun C F, et al. *Cryst. Growth Des.*, **2012**,**12**:1337-1346
- [30]Xia J, Wang H S, Shi W, et al. *Inorg. Chem.*, **2007**,**46**:3450-3458
- [31]Nakamoto K, Translated by HUANG De-Ru(黄德如), WANG Ren-Qing (汪仁庆). *Infrared Raman Spectra of Inorganic and Coordination Compounds*(无机和配位化合物的红外和拉曼光谱). Beijing: Chemical Industry Press, **1986**:235
- [32]Li D X, Chen M M, Li F L, et al. *Inorg. Chem. Commun.*, **2013**,**35**:302-306
- [33]Zhang L Y, Liu G F, Zheng S L, et al. *Eur. J. Inorg. Chem.*, **2003**:2965-2971
- [34]Wang X L, Qin C, Wang E B, et al. *Angew. Chem. Int. Ed.*, **2004**,**43**:5036-5040